Online calibration, particle ID, and analysis for FAUST and other large multi-detector arrays in nuclear physics

A.B. McIntosh, A. Hannaman, and K. Hagel

An experiment to measure products from ^{28}Si + ^{12}C collisions at 35MeV/u using the Forward Array Using Silicon Technology (FAUST) [1-3] was recently conducted. A new "multi-event" [4] readout was deployed to dramatically reduce deadtime and allow high counting rate. This readout required accurate time stamping of digitized data which must be subsequently time-matched. In principle, the observation of isotopic lines in the *ΔE-E* plots indicates that this is being achieved to some degree. But since the measurement was aimed at looking for the high-multiplicity 7-α breakup of excited "toroidal" states in ^{28}Si, data packet matching must be working correctly and very efficiently. To this end, I developed a new online calibration and particle ID toolset as additional verification early in the experiment that the data was being recorded as desired. This toolset can be adapted and deployed for other multi-detector arrays.

First, the energy calibration of the silicon detectors was established using a ^{229}Th source (any multi-line source would work). These are fit automatically with a multi-gaussian function which assumes all peaks have the same width, and that the spacing between the peaks given by the true energies, modified by the dead layers, is preserved modulo a gain and offset. All peak amplitudes are independent. Thus for N peaks the function has N+3 degrees of freedom. (I had recently built this functionality for the silicon detector of DAPPER). Fig. 1 shows a typical spectrum with resulting fit. The gain and offset from the fit constitutes the linear calibration of the silicon detector.

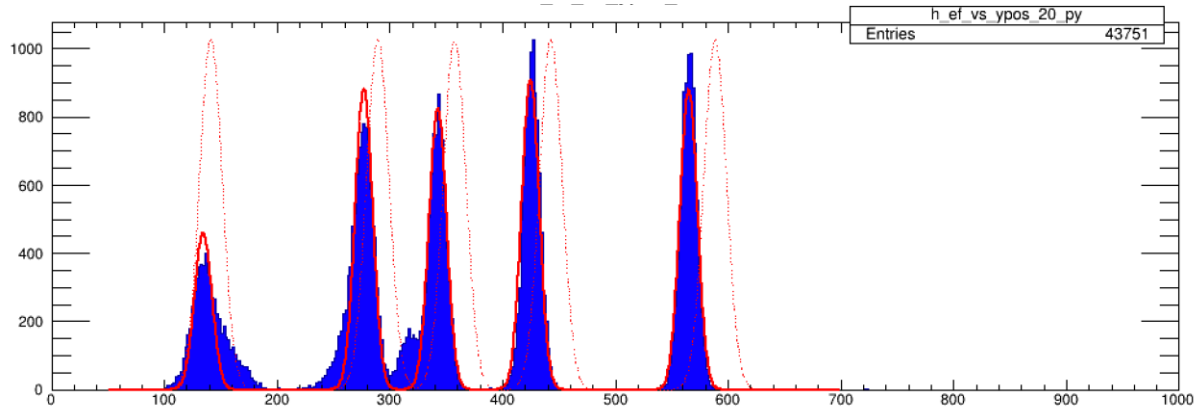

Fig. 1. ^{229}Th spectrum (blue), initialization of multi-gaussian function (dashed red) and resulting multi-gaussian fit (solid red); the last constitutes the online calibration.

Second, particle ID must be done, as the CsI cannot be accurately calibrated without it. Since the spectrum of ΔE vs E exhibits points along a locus described (approximately) by hyperbolas, plotting the data in log-log scale gives (approximately) straight lines. For our purposes, identification of alpha particles is most important and, fortunately, easiest. The log-log distribution is shown in Fig. 2 in black, the dominant yield is alpha particles. The profile, <log(ΔE)> vs log(E) is shown in blue and is fit with a line. A narrow selection around this line allows selection of alpha particles with some contamination,

mostly from 3He. Thus, sufficient particle ID is achieved for online high-multiplicity alpha particle analysis.

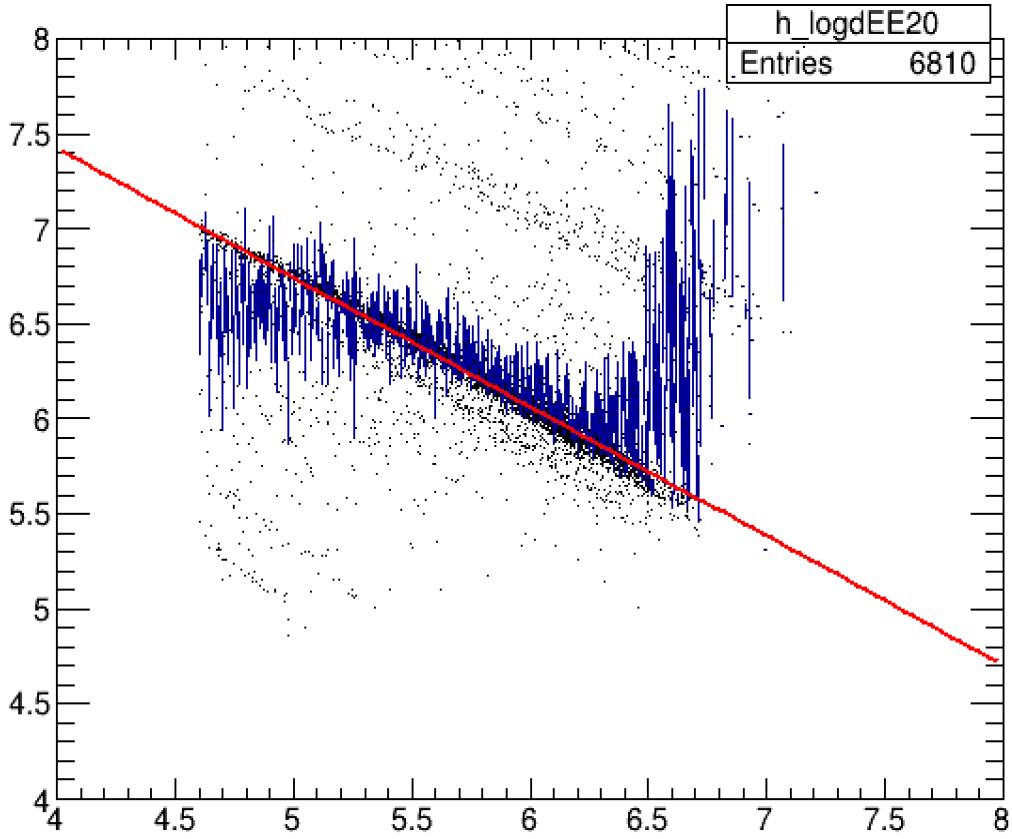

Fig. 2. log(ΔE) vs log(E) in black. The profile, <log(ΔE)> vs log(E) is shown in blue and fit with a linear function. The vertical distance to this function constitutes the particle ID parameter, and a gate of constant width around this red line selects only alpha particles (with some 3He contamination).

Next, the CsI detectors are calibrated using the known energy in the silicon, the thickness of the silicon, the particle type (just alpha particles) and energy loss calculations (using CycSrim [5,6]). The deduced energy deposited in the CsI is nearly linear as a function of the measured signals from the CsI detector, and a fit to this correlation comprises the CsI energy calibration.

The position of each particle is determined as in the previous FAUST-DADL experiments, using the known positions of the detectors, and the four signals from each silicon to establish the local position within each silicon detector [3]; the local scaling parameters were increased to adjust for the use of the long integration of the signals [7]. To check the position calibration, a precision slotted mask was placed between a collimated source and the detectors; stripes were observed across the global position projection as expected as shown in Fig. 3.

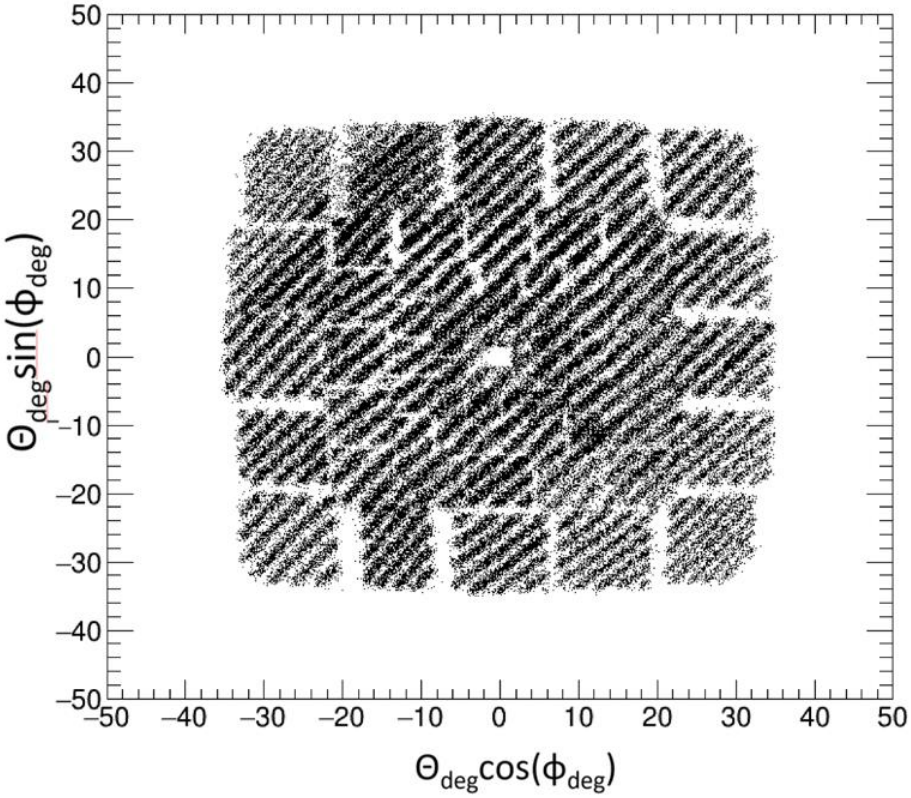

Fig. 3. Global position projection (φ sin(θ) vs φ cos(θ)) obtained from a collimated ^{229}Th source with the precision slotted mask.

This calibration allowed us see, online, ^{8}Be(gs,3.03), ^{9}Be(2.43MeV), and ^{12}C(7.6, 9.6) peaks in relative energy distributions shown in Fig. 4, and to verify that the relative energy distribution for 7-alpha

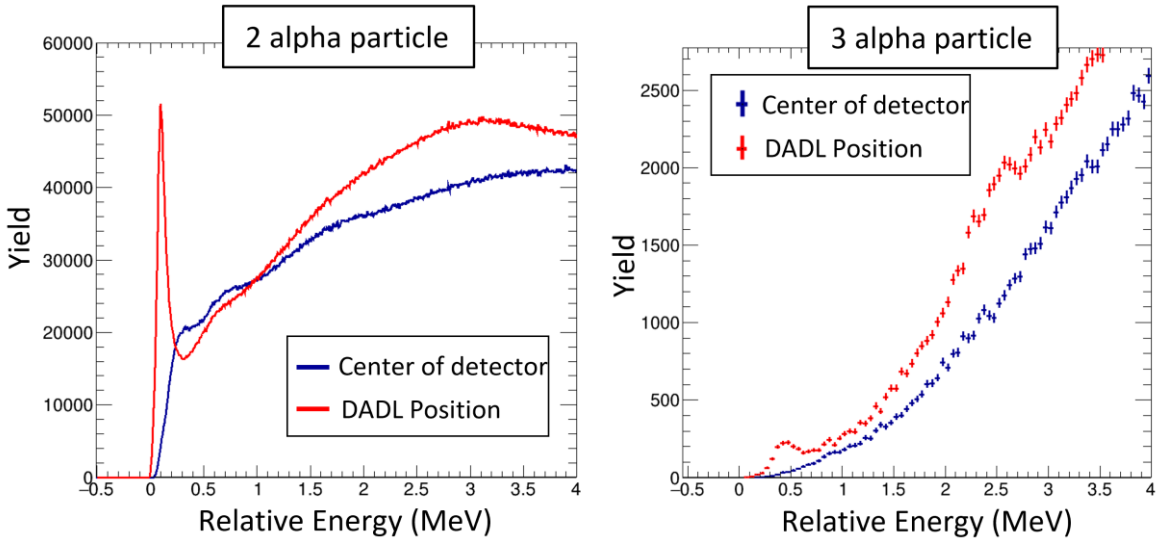

Fig. 4. Preliminary relative energy distributions for two alpha particles (left) and three alpha particles (right) for true events (red) and mixed events (blue) obtained with the quick online calibration and analysis toolkit.

events in fact covered a similar energy range as the previous NIMROD experiment in which possible signals of toroidal states were observed [8]. It also allowed us to see that for all alpha multiplicities, the energy per nucleon of the center of mass of all measured alpha particles (shown in Fig. 5) was peaked between 22-24 MeV, significantly damped from beam energy of 35 MeV/u, suggesting incomplete fusion as a significant reaction mechanism.

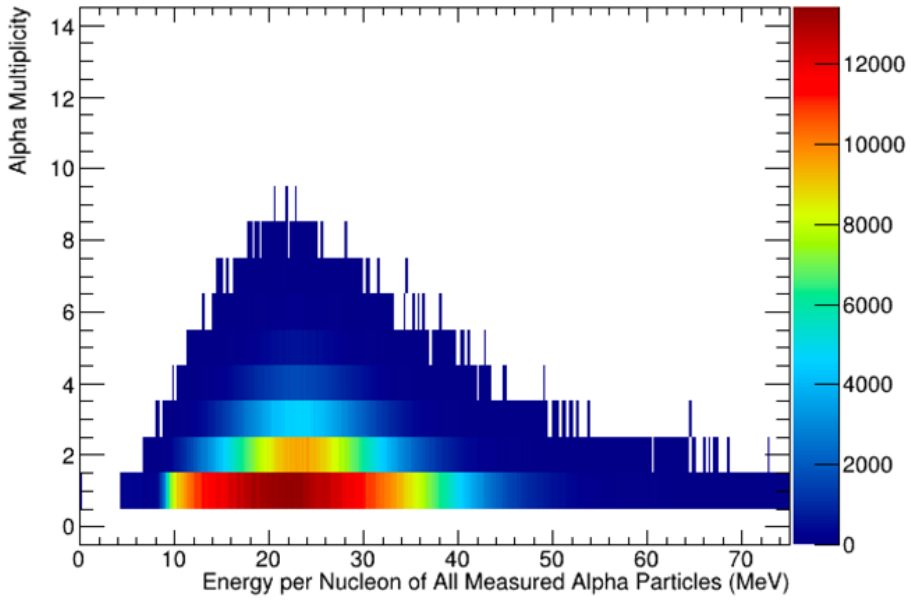

Fig. 5. Alpha multiplicity vs total energy per nucleon of all alpha measured particles. Significant damping from beam energy suggests incomplete fusion may be dominant.

Further development of online particle ID is the limiting step to a more complete online analysis, and investigation into an automated method of that is underway both for identification of Z and possibly A. At present, this online tool package has succeeded in indicating that the present high-rate data set obtained with multi-events does preserve the physical events, packaging them, at least to a large extent, into proper corresponding data events.

[1] F. Gimeno-Nogues, D.J. Rowland, E. Ramakrishnan, S. Ferro, S. Vasal, R.A. Gutierrez, R. Olsen, Y.-W. Lui, R. Laforest, H. Johnston, and S.J. Yennello, Nucl. Instrum. Methods Phys. Res. **A399**, 94 (1997).

[2] S.N. Soisson, B.C. Stein, L.W. May, R.Q. Dienhoffer, M. Jandel, G.A. Souliotis, D.V. Shetty, S. Galanopoulos, A.L. Keksis,S. Wuenschel, Z. Kohley,S.J. Yennello, M.A. Bullough, N.M. Greenwood, S.M. Walsh, and C.D. Wilburn, Nucl. Instrum. Methods Phys. Res. **A613**, 240 (2010).

[3] L.A. McIntosh, A.B. McIntosh, K. Hagel, M.D. Youngs, L.A. Bakhtiari, C.B. Lawrence, P. Cammarata, A. Jedele, L.W. May, A. Zarrella, and S.J. Yennello, Nucl. Instrum. Methods Phys. Res. **A985**, 164642 (2020).

[4] K. Hagel *et al.*, *Progress in Research*, Cyclotron Institute, Texas A&M University (2020-2021), p. V-58.
[5] L.C. Northcliffe and R.F. Schilling, Nucl. Data Tables **A7**, 233 (1970).
[6] F. Hubert, R. Bimbot, and H. Gauvin, At. Data Nucl. Data Tables, **46**, 1 (1990).
[7] M.W. Aslin, A. Hannaman, M.D.Youngs, A.B.McIntosh, A. Abbott, P.Adamson, J. Gauthier, K.Hagel, A.Jedele, Y.-W.Lui, L.A.McIntosh, M.Q.Sorensen, Z.N.Tobin, R.Wada, A.Wakhle, and S.J. Yennello, Nucl. Instrum. Methods Phys. Res. **A985**, 164674 (2020).
[8] X. G. Cao, E. J. Kim, K. Schmidt, K. Hagel, M. Barbui, J. Gauthier, S. Wuenschel, G. Giuliani, M. R. D. Rodriguez, S. Kowalski, H. Zheng, M. Huang, A. Bonasera, R. Wada, N. Blando, G. Q. Zhang, C. Y. Wong, A. Staszczak, Z. X. Ren, Y. K. Wang, S. Q. Zhang, J. Meng, and J. B. Natowitz, Phys. Rev. C **99**, 014606 (2019).

.